ACS Chemical Neuroscience

Research Article

pubs.acs.org/chemneuro

Kinetic Analysis Reveals the Identity of Aβ-Metal Complex Responsible for the Initial Aggregation of Aβ in the Synapse

Thomas Branch,[†,‡] Mauricio Barahona,[†,§] Charlotte A. Dodson,[∥] and Liming Ying*[,†,∥]

[†]Institute of Chemical Biology, [‡]Department of Chemistry, [§]Department of Mathematics, and [∥]National Heart and Lung Institute, Imperial College London, London SW7 2AZ, United Kingdom

Supporting Information

ABSTRACT: The mechanism of Aβ aggregation in the absence of metal ions is well established, yet the role that Zn^{2+} and Cu^{2+}, the two most studied metal ions, released during neurotransmission, paly in promoting Aβ aggregation in the vicinity of neuronal synapses remains elusive. Here we report the kinetics of Zn^{2+} binding to Aβ and Zn^{2+}/Cu^{2+} binding to Aβ-Cu to form ternary complexes under near physiological conditions (nM Aβ, μM metal ions). We find that these reactions are several orders of magnitude slower than Cu^{2+} binding to Aβ. Coupled reaction-diffusion simulations of the interactions of synaptically released metal ions with Aβ show that up to a third of Aβ is Cu^{2+}-bound under repetitive metal ion release, while any other Aβ-metal complexes (including Aβ-Zn) are insignificant. We therefore conclude that Zn^{2+} is unlikely to play an important role in the very early stages (i.e., dimer formation) of Aβ aggregation, contrary to a widely held view in the subject. We propose that targeting the specific interactions between Cu^{2+} and Aβ may be a viable option in drug development efforts for early stages of AD.

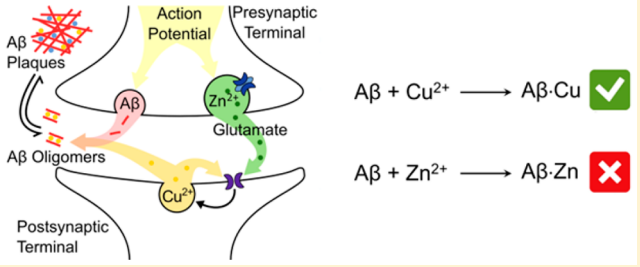

KEYWORDS: *Kinetics, stopped-flow, fluorescence, reaction-diffusion simulation, amyloid-β-metal ion complex, neuronal synapse*

INTRODUCTION

The accumulation of amyloid-β (Aβ) peptides into amyloid plaques is one of the pathological hallmarks of Alzheimer's disease (AD).[1,2] High contents of metal ions such as zinc and copper colocalize with amyloid plaques, prompting to the study of the role of metal ions in Aβ aggregation or toxicity.[3,4] Aβ oligomers are widely regarded as the most toxic species relating to AD.[5,6] Recent work has further demonstrated that different pathological Aβ conformers can seed additional aggregates with the same shape, and this defines different strains of the disorder,[7,8] similar to prion diseases. These observations raise the question of how Aβ oligomers form in the brain. The mechanism of Aβ aggregation in the absence of metal ions is well established: a slow primary nucleation is followed by a fast secondary nucleation-catalyzed fibrillization process.[9,10] However, the effect of metal ions on the aggregation pathways and kinetics is still poorly understood despite extensive studies.[11−16] Even a trace amount of metal ions in common buffers has been shown to initiate Aβ aggregation,[17] making experimental results difficult to compare. Further investigations into the roles and mechanisms that govern the formation and toxicity of metal loaded Aβ seeds under near physiological conditions are therefore urgently needed.

The resting level of free Zn in the extracellular fluid is approximately 20 nM,[18] whereas the normal brain extracellular concentration of Cu is 0.2−1.7 μM.[19] (For simplicity, we use Zn and Cu to represent Zn^{2+} and Cu^{2+} throughout.) The Cu ions are normally tightly bound to Cu enzymes or proteins, e.g., cytochrome *c* oxidase, ceruloplasmin, and superoxidase dismutase. Therefore, it is unlikely that physiological concentrations of Aβ and freely exchangeable Zn and Cu in the brain would be able to promote primary nucleation via metal ion binding. However, the concentration of labile Zn or Cu in the neuronal synaptic cleft can transiently reach levels of up to 100 μM upon the release of these ions during neuronal excitation.[20,21] This concentration is higher than the equilibrium dissociation constant of both Aβ-Zn (1−100 μM) and Aβ-Cu (0.1−1 nM) complexes.[22−24] From a thermodynamic perspective, it is thus believed that both Zn and Cu are involved in the aggregation of Aβ in AD.[3,4,12,25−28] Furthermore, it has been reported[29,30] that Zn alters the Cu coordination environment in mixed Zn-Aβ-Cu ternary complexes. This may have implications for Aβ aggregation and redox activity, although the impact on Aβ-Cu-induced ROS production has not yet been confirmed.[31] The direct involvement of Zn and Cu in the early molecular events of aggregation, such as dimerization and small oligomeric "seed" formation, in the synaptic cleft has not been addressed, though there is evidence that synapses are the sites where physiological Aβ starts to accumulate and aggregate.[32] The spatiotemporal profile of the metal ion release during neuronal spiking is expected to have a strong effect on the metal binding reactions within the cleft,

Received: April 4, 2017
Accepted: June 16, 2017
Published: June 16, 2017

DOI: 10.1021/acschemneuro.7b00121
ACS Chem. Neurosci. 2017, 8, 1970−1979

prompting the need for a reaction-diffusion analysis following the experimental characterization of the elementary binding reactions.

We have previously developed and applied an ultrasensitive method to measure the kinetics of the interactions between Cu and Aβ.[33,34] In this paper, we examine the kinetics of Zn binding to Aβ as well as Zn and Cu binding to Aβ-Cu to form ternary complexes under near physiological conditions (nM Aβ, μM metal ions). We then carry out reaction-diffusion simulations on the interactions of synaptically released metal ions with Aβ. We find that a significant proportion of Aβ is Cu-bound under repetitive metal ion release during neurotransmission, while the amount of Zn-bound Aβ is negligible. Based on these results we propose that, contrary to the widely held belief in the literature,[3,4,12,25−28] Zn-bound Aβ species are unlikely to play an important role in the very early steps of Aβ aggregation, such as dimer formation. Nevertheless, Zn is likely to be involved in the late stages of Aβ aggregation when the affinity of its binding to protofibrils and fibrils increases.

RESULTS AND DISCUSSION

Kinetics of Zn Binding to Aβ. We previously used divalent Cu-induced quenching of a fluorescent dye attached to the C-terminus of Aβ to show that the binding of Cu to both Aβ_{16} and Aβ_{40} is nearly diffusion-limited at $\sim 5 \times 10^8$ M^{-1} s^{-1}.[33] The detailed kinetic parameters (e.g., interconversion rates between two different coordination modes) of Cu-association with Aβ_{16} and Aβ_{40} are very similar and therefore we decided to use Aβ_{16} as a model system for further kinetics studies. As Zn does not directly quench the fluorophore attached to Aβ, a competition experiment is required to determine the kinetics of Zn binding by fluorescence. We did not use a Zn indicator as this would require μM concentration of Aβ to compete with it while still remaining under pseudo-first-order reaction conditions. Such high concentrations would inevitably cause Aβ aggregation in the presence of metal ions (dimerization rate constant on the order of 10^5 M^{-1} s^{-1} as determined in our previous work[34]). Instead, we used labeled Aβ and let Zn and Cu compete to bind to the peptides. All the kinetics measurements were carried out under pseudo-first-order conditions, such that [Zn] $\gg$ [Aβ] and [Cu] $\gg$ [Aβ]. This enables the reaction scheme to be solved analytically.

Scheme 1 illustrates the reaction model that we considered (see Supporting Information). In this scheme we have only

Scheme 1

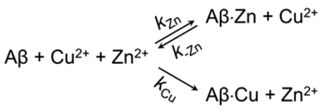

included those reactions expected to occur at rates not much slower than the experimentally observed rates between 20 s^{-1} and 100 s^{-1} under our experimental conditions. Therefore, we have excluded all reactions involving the Zn·Aβ·Cu triple complex, coordination of second (and subsequent) Cu ions and further reaction of Zn with Aβ·Zn. The expected rate for the reaction Aβ·Cu + Zn^{2+} → Zn·Aβ·Cu is 0.6 s^{-1} at the highest concentration of Zn used in these experiments (rate constant determined to be 3×10^3 M^{-1} s^{-1} in Kinetics of Zn Binding to Aβ-Cu subsection). The related reaction Aβ·Zn + Cu^{2+} → Zn·Aβ·Cu is also excluded because a rate constant of 2×10^6 M^{-1} s^{-1} or greater is required for the reaction to have a rate of at least 1 s^{-1} in our experiments. This is unlikely given that the rate constants for the reaction Aβ·Cu + Zn^{2+} → Zn·Aβ·Cu and Aβ·Cu + Cu^{2+} → Cu·Aβ·Cu are 3×10^3 and 1×10^5 M^{-1} s^{-1} respectively. From these rate constants, the latter reaction is also too slow to participate in our chosen time regime (0.05 s^{-1}). The reaction of Zn with Aβ·Zn is also excluded by the same reasoning.

To determine the kinetics of Zn binding, $CuCl_2$ was premixed with various concentrations of $ZnCl_2$, which were then mixed with dye-labeled Aβ using stopped-flow (original traces in Figure 1A). Raw data was fitted to a double

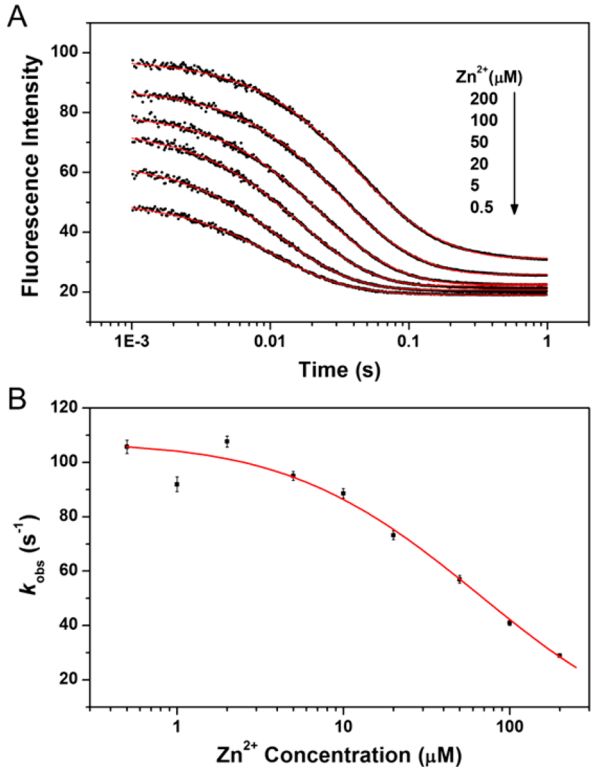

Figure 1. Kinetics of Zn binding to Aβ determined by a competition assay. (A) Representative raw kinetic traces of Cu (250 nM) binding to Aβ (12.5 nM) in the presence of Zn with concentrations of 0.5, 20, 50, 100, and 200 μM. The red solid lines are fits to a double exponential function. Note log scale on *X*-axis. (B) Observed reaction rate constants as a function of Zn concentration. The solid line is the fit to eq 5 in the Supporting Information.

exponential function and the observed rate constant of the fast phase was plotted as a function of Zn concentration (Figure 1B). The Zn-dependence of this observed rate constant was then fitted to eq 5 (details of equation and derivation in the Supporting Information) and from the data fit, k_{Zn} was determined to be $1.9 \pm 0.3 \times 10^6$ M^{-1} s^{-1} and K_d ($=k_{-Zn}/k_{Zn}$) to be 58 ± 9 μM. Therefore, k_{-Zn} is 110 ± 20 s^{-1}. The fitted value for k_{Cu} was 160 ± 20 s^{-1}, in agreement with the value from our previous direct measurement of Cu binding to Aβ,[33] while K_d is in broad agreement with the expected range from the literature (1 μM to 100 μM).[20,22,24,35,36] Strikingly, k_{Zn} is approximately 2 orders of magnitude smaller than the association rate constant of Cu with Aβ under the same conditions. Furthermore, the dissociation rate constant k_{-Zn} corresponds to a lifetime of 9 ms for the Aβ-Zn complex,

DOI: 10.1021/acschemneuro.7b00121
ACS Chem. Neurosci. 2017, 8, 1970−1979

approximately 150 times shorter than that of the Aβ-Cu complex (~1.3 s), suggesting that Aβ-Zn is kinetically much less stable.

Kinetics of Zn Binding to Aβ-Cu. It has been suggested that Zn-Aβ-Cu ternary complex may be relevant in AD.[29−31] Zn has been shown to substantially perturb Cu coordination with Aβ;[29−31] however, no effect has been observed on Aβ-Cu-induced ROS production and associated cellular toxicity.[31] As the Aβ-Cu complex survives long enough for the presynaptically released Zn to bind during sustained neuronal stimulation, we decided to carry out double-jump stopped-flow experiments to establish the association kinetics of Zn with Aβ-Cu by displacing Cu with Zn via a ternary complex intermediate Zn-Aβ-Cu as illustrated in Scheme 2.

Scheme 2

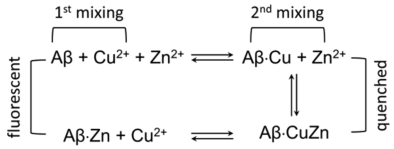

In our initial experiments, Aβ was first mixed with $CuCl_2$ and subsequently with excess $ZnCl_2$. Two exponential phases were observed, with apparent rate constants independent of Zn concentration. Our measured fluorescence signal arises from the release of Cu and the rate constant of the slow dominant phase ($0.47 \pm 0.3\ s^{-1}$) was the same as that of the spontaneous dissociation of the Aβ-Cu complex, suggesting that this phase does not contain useful information on the Zn interaction with Aβ-Cu. We therefore hypothesized that the observed rate constant of the faster minor phase ($5.2 \pm 0.2\ s^{-1}$; Figure 2A) was related to the dissociation of Zn-Aβ-Cu complex.

To find whether we could perturb the relative reaction rates, we then measured the temperature dependence of the reaction of Aβ-Cu complex with Zn (Figure 2B). The Arrhenius plot of the apparent rate constant of the fast phase indicates a change in the slope at 34 ± 2 °C. This suggests that for temperatures above this critical point, there is a change in the rate limiting process. To determine the Zn-dependence of this reaction, Aβ-Cu was reacted with 100 to 300 μM Zn at temperatures between 35 and 55 °C. The rate constants of the fast phase were indeed dependent on the concentration of Zn (Figure 2C) and the second-order association rate constants obtained from the gradients were then plotted against the temperature (Figure 2D). Extrapolating to 25 °C gave a binding rate constant of $3 \pm 1 \times 10^3\ M^{-1}\ s^{-1}$. The activation energy for the binding was determined to be 106 ± 19 kJ mol^{-1}. Considering that when Zn is bound, Cu lies more in much more stable Component II coordination,[30] the dissociation rate of Cu from the ternary complex would be at least as slow as that from the

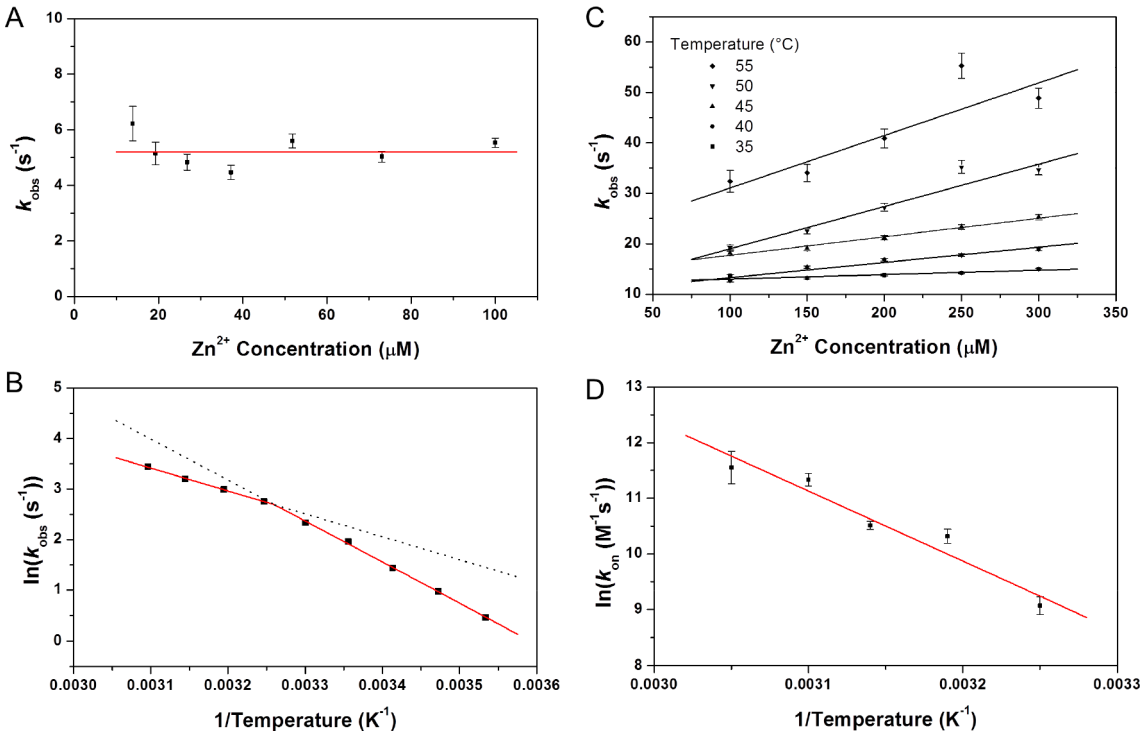

Figure 2. Zn binding to Aβ-Cu complex. (A) Observed rate constants of the fast phase of the displacement of Cu are independent of Zn concentration at 298 K (25 °C) and have a mean value of $5.2 \pm 0.2\ s^{-1}$ (solid line). (B) Arrhenius plot of labeled Aβ-Cu reacting with 300 μM $ZnCl_2$. The solid lines and the extended dotted lines are a linear fit to $\ln(k_{obs}) = \begin{cases} T^{-1} \le \dfrac{R(c_1 - c_2)}{E_{a1} - E_{a2}}, & c_1 - \dfrac{E_{a1}}{RT} \\ \text{otherwise}, & c_2 - \dfrac{E_{a2}}{RT} \end{cases}$, where k is the apparent rate; T is temperature; R is the ideal gas constant; c_1, c_2 are the natural logarithms of the pre-exponential factors; and E_{a1}, E_{a2} are the activation energies. The intersection of the two lines is at 307 ± 2 K (34 ± 2 °C). (C) Observed reaction rate constants are dependent on Zn concentration when the temperature is higher than 34 °C. (D) Temperature dependence of the association rate constant (k_{on}), determined from the gradient of the fits in (C).

DOI: 10.1021/acschemneuro.7b00121
ACS Chem. Neurosci. 2017, 8, 1970−1979

Aβ-Cu binary complex. We therefore estimated the equilibrium dissociation constant for the Zn-Aβ-Cu complex to be ~2 mM (using 5.2 s^{-1} as the rate constant of Zn dissociation from the complex), suggesting that this mixed Aβ-metal complex is unlikely to form in the vicinity of synapse.

Multiple Cu Binding to Aβ. Aβ can bind up to four Cu ions at its N-terminus.[37] We previously observed that, at low Cu concentration (<200 nM), only one quenching phase occurred which was attributed to the binding of one Cu ion.[33] However, once the Cu concentration is higher than 1 μM, further quenching phases with smaller amplitudes were detected. These phases are independent of the Aβ concentration, therefore they could be attributed to Aβ binding to more Cu ions, but not Aβ aggregation. Under these Cu concentrations the first Cu binding is not detectable as it finishes within the dead-time of the stopped flow instrument. To investigate the binding kinetics of the second Cu ion to Aβ, reactions of dye labeled Aβ with 5 to 20 μM $CuCl_2$ were measured to obtain the apparent association rate constants (Figure 3A). We fitted the Cu-dependence of this to a linear equation and determined the association rate constant of the second Cu, k_{on}, to be 4.2 ± 0.6 × 10^5 M^{-1} s^{-1} and the dissociation rate constant, k_{off}, to be 7.3 ± 0.7 s^{-1}. The equilibrium dissociation constant K_d is therefore 17 ± 3 μM, which is in good agreement with ~10 μM obtained using both ITC and fluorescence.[38]

To further probe the binding of multiple copper to Aβ, again a double mixing approach was employed. Labeled Aβ was premixed with various concentrations of $CuCl_2$ and the solutions were then mixed with an equal volume of 4 mM EDTA to compete with Aβ for Cu binding. The resulting fluorescence recovery traces were globally fitted with multiple exponentials sharing the rates across data sets. Five species (I–V) were identified based on their pseudo-first-order reaction rate constants with the EDTA (Figure 3B and C). The first two species (Types I and II) have the same reaction rate constants with EDTA as Component I ($(Aβ\text{-}Cu)_I$) and Component II ($(Aβ\text{-}Cu)_{II}$) Aβ-Cu complexes and accordingly were assigned to these two complexes,[33] while the remaining three species were tentatively assigned to Aβ-Cu complexes with two to four bound Cu ions (Types III–V).

Simulation of Cu/Zn Binding to Aβ during Synaptic Transmission. Having determined the reaction rate constants between Aβ and metal ions, we carried out reaction-diffusion simulations to study the relative importance of the different possible binding reactions in the synaptic cleft during neurotransmission (for details, see the Supporting Information). In our simplified model of the synapse (Figure 4A), we considered diffusion within a cylinder of infinite width (to mimic the possibility that metal ions can diffuse beyond the synapse) and constant height of 20 nm (the height of synapses vary between 10 to 25 nm[39]). Metal ions (30 μM Cu or 300 μM Zn) were assumed to be released at the center of the synapse (i.e., the center of the cylinder) via 40 nm diameter vesicles,[40] and allowed to diffuse freely (diffusion coefficients D_{Zn} = D_{Cu} = 650 nm^2 $μs^{-1}$)[41] and to react with 3 nM Aβ[42] (diffusion coefficient of $D_{Aβ}$ = 304 nm^2 $μs^{-1}$ determined by our own fluorescence correlation spectroscopy measurement) or 5 μM HSA (D_{HSA} = 61 nm^2 $μs^{-1}$).[43] The diffusion coefficients of the Aβ-metal and HSA-metal complexes were set to be the same as those of Aβ and HSA respectively. Although more detailed fully stochastic simulations could be performed, the reaction-diffusion numerics provide a first evaluation of the relevance of the different reactions involved.

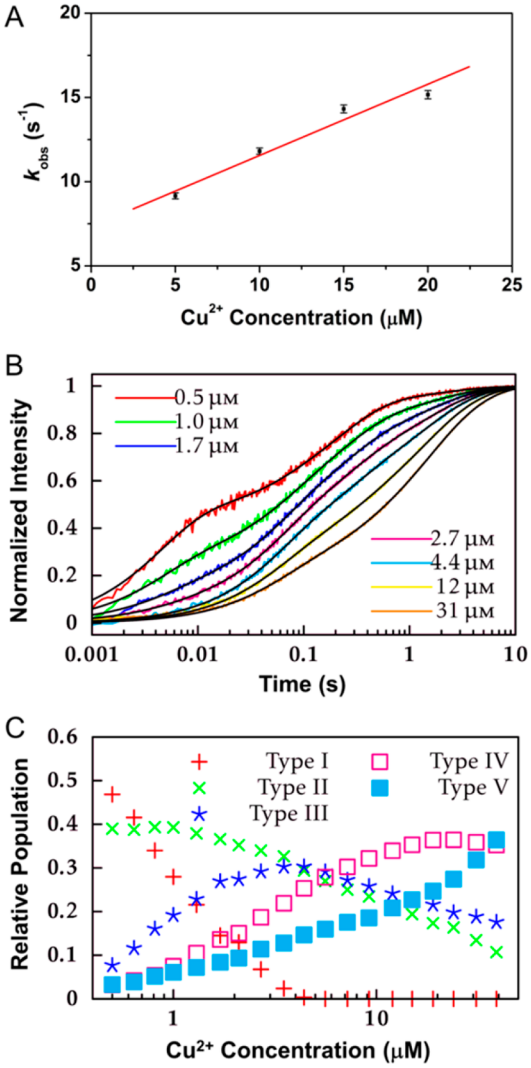

Figure 3. Kinetics of multiple Cu binding to Aβ. (A) Observed reaction rate constant as a function of Cu concentration for the second Cu binding event. (B) Normalized fluorescence recovery traces for the reaction of EDTA with Aβ-Cu complexes formed at indicated Cu concentrations. The five apparent reaction rates derived from the fit are k_I = 234 ± 4 s^{-1}, k_{II} = 4.46 ± 0.03 s^{-1}, k_{III} = 19.9 ± 0.2 s^{-1}, k_{IV} = 0.845 ± 0.009 s^{-1}, and k_V = 0.331 ± 4 s^{-1}. (C) Relative populations of the five species identified in (B) as a function of Cu concentration.

We first simulated the binding of metal ions (Cu/Zn) to Aβ during a single synaptic release. We considered the binding reactions for one and two Cu ions as well as Cu dissociation and interconversion between species using rate constants determined above and elsewhere[33] (Figure 4B). During one release, the Cu concentration drops more than 3 orders of magnitude within 1 ms (Figure 4C). Approximately 0.1% of the total Aβ is expected to react with Cu to form a complex on time scales of 1 μs-10 ms. Most of this complexification is in the form of $(Aβ\text{-}Cu)_I$ (Figure 4D), with $(Aβ\text{-}Cu)_{II}$ reaching approximately 0.01% at time scales of 0.3 ms to tens of millisecond (Figure 4E). Under thermodynamic equilibrium, the ratio of $(Aβ\text{-}Cu)_I$ to $(Aβ\text{-}Cu)_{II}$ is approximately 71:29, but in the dynamic conditions experienced in the synaptic cleft the kinetics favors $(Aβ\text{-}Cu)_I$ which forms first after Cu binding. In

DOI: 10.1021/acschemneuro.7b00121
ACS Chem. Neurosci. 2017, 8, 1970–1979

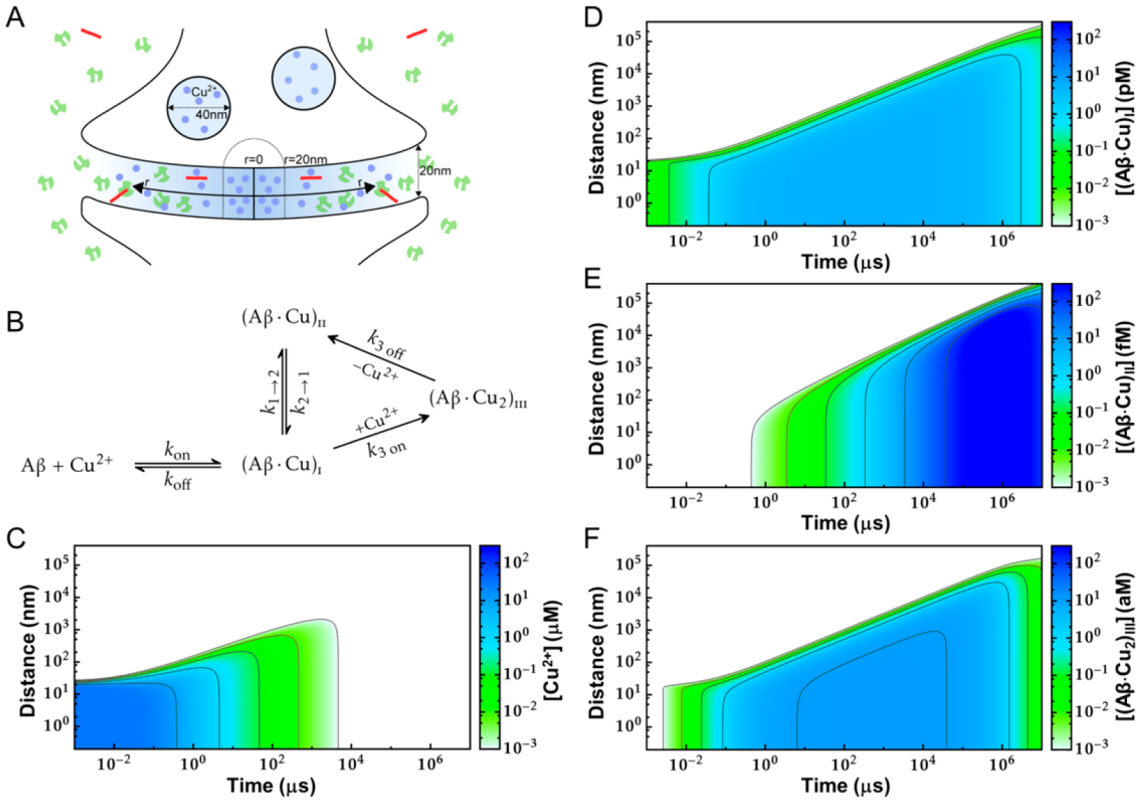

Figure 4. Reaction-diffusion simulation of Cu binding to Aβ in the synaptic cleft. (A) Schematic of the Cu release into the synaptic cleft from a 40 nm diameter vesicle. The red lines and the small blue circles represent Aβ and Cu, respectively. The synapse is approximated as a cylinder with a height of 20 nm. (B) The reaction scheme used for the simulation, with reaction rate constants used are $k_{on} = 3.0 \times 10^8$ M^{-1} s^{-1}, $k_{off} = 0.8$ s^{-1}, $k_{1\to2} = 0.9$ s^{-1}, $k_{2\to1} = 2.22$ s^{-1}, $k_{3\ on} = 4.2 \times 10^5$ M^{-1} s^{-1}, and $k_{3\ off} = 1.7$ s^{-1} (C−F) Spatiotemporal profiles of the concentration of the chemical species Cu, $(A\beta{\cdot}Cu)_I$, $(A\beta{\cdot}Cu)_{II}$, and $(A\beta{\cdot}Cu_2)_{III}$ from simulation of 30 μM Cu released from the vesicle at the center of the synapse ($r = 0$) at time $t = 0$ and reacting with 3 nM Aβ. The contours correspond to the molar concentrations that are powers of 10.

contrast, $(A\beta\text{-}Cu_2)_{III}$ only reaches tens of attomolar concentrations (approximately 10^{-6}% of total Aβ), on millisecond time scales (Figure 4F). Similarly, Aβ-Zn only reaches a concentration of hundreds of attomolar across time scales of 0.5 μs to 30 ms (Figure 5; approximately 10^{-5}% of total Aβ).

We next simulated the effect of human serum albumin (HSA) on the binding of Cu to Aβ (Figure 6). HSA is at micromolar concentrations in the cerebrospinal fluid and binds quickly and strongly to Cu.[33,44] It has been suggested that HSA might be a guardian against Cu/Aβ toxicity in extracellular brain compartments.[45] It is known that the binding of HSA to Cu cannot compete efficiently with Aβ on short time scales (<100 ms), and so we previously estimated the binding rate constant, k_{HSA}, to be $\sim 1 \times 10^8$ M^{-1} s^{-1}.[33] Dissociation of Cu from the HSA-Cu complex was ignored, as this would take much longer than the time scale of the simulation. The inclusion of HSA into the model has little effect on the transient maximal concentration of $(A\beta\text{-}Cu)_I$ but reduces the highest transient concentration of $(A\beta\text{-}Cu)_{II}$ by a factor of 60 (Figure 6A and B). However, HSA has a noticeable effect on the temporal profiles: in the absence of HSA, $(AB\text{-}Cu)_I$ is maintained at concentrations above picomolar for at least 1000 ms; in the presence of HSA, $(AB\text{-}Cu)_I$ falls below picomolar concentrations after ~10 ms, a reduction in duration of approximately 2 orders of magnitude.

In the brain, neurons fire multiple times releasing metal ions into the synapse in quick succession. We wondered how the repeated firing of neurons would affect the spatiotemporal profile of the different Aβ species and, in particular, whether Aβ-Zn would build up from sustained releases during neurotransmission. The upper firing frequency of neurons is approximately 200 Hz,[46] so we explored a range of 1−100 Hz in our simulation (Figures 7 and S1−S3). Across the frequency range simulated, repetitive metal release caused an increase in the concentration of $(A\beta\text{-}Cu)_I$ (Figures 7A and S1) relative to $(A\beta\text{-}Cu)_{II}$ (Figures 7B and S2), a factor of more than 3 compared to 2.47 expected at equilibrium. There was little increase in the maximum transient concentration of the Aβ-Zn complex since it dissociates quickly (dissociation rate constant 110 s^{-1}) (Figures 7C and S3). The mean concentrations of Aβ-metal complexes across the entire synapse (300 nm width) rise with increasing metal ion release frequency (Figure 7D). Sizeable $(A\beta\text{-}Cu)_I$ (0.8 nM) and $(A\beta\text{-}Cu)_{II}$ (0.26 nM) concentrations were reached at 100 Hz, which are equivalent to 27% and 9% respectively of the total Aβ concentration. On the other hand, the concentration of Aβ-Zn reached only low picomolar concentrations by the end of the simulation (10 s), approximately 0.1% of the total Aβ concentration. These results indicate that Aβ binds to Cu released during neurotransmission, whereas Zn-bound Aβ is very rare. A substantial buildup of Aβ-Zn is not observed even under sustained Zn release.

DISCUSSION

At equilibrium, both Cu and Zn bind to Aβ when metal ion concentrations are on the order of tens of micromolar. The situation is very different in the dynamic synapse. Our reaction-

DOI: 10.1021/acschemneuro.7b00121
ACS Chem. Neurosci. 2017, 8, 1970−1979

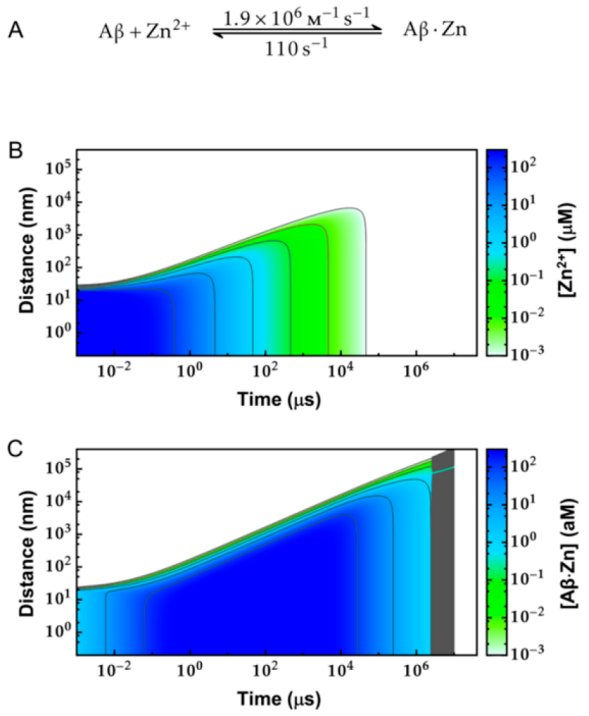

Figure 5. Reaction-diffusion simulation of Zn binding to Aβ in the synaptic cleft. 300 μM Zn was released from a 40 nm diameter vesicle and reacted with 3 nM Aβ. (A) Reaction scheme used in the simulation. (B) Zn and (C) Aβ·Zn concentrations as a function of time and distance. The contour lines correspond to the molar concentrations that are powers of 10. The black region is due to occasional numerical instability in the simulation.

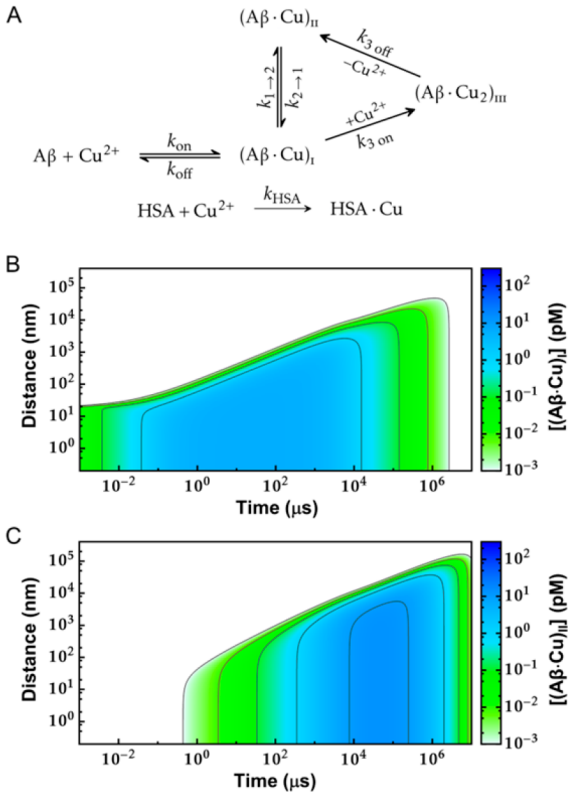

Figure 6. Reaction-diffusion simulation of Cu binding to Aβ in the presence of HSA in the synaptic cleft. (A) Reaction scheme. (B, C) Spatiotemporal profiles of (B) $(A\beta\text{-Cu})_I$ and (C) $(A\beta\text{-Cu})_{II}$. In the simulation 30 μM Cu was released from a 40 nm diameter vesicle into a reservoir of 5 μM HSA and 3 nM Aβ. The contour lines correspond to the molar concentrations that are powers of 10. The rate constants used are $k_{on} = 3 \times 10^8$ M^{-1} s^{-1}, $k_{off} = 0.8$ s^{-1}, $k_{1\to2} = 0.9$ s^{-1}, $k_{2\to1} = 2.22$ s^{-1}, $k_{3on} = 4.2 \times 10^5$ M^{-1} s^{-1}, $k_{3off} = 1.7$ s^{-1}, and $k_{HSA} = 1 \times 10^8$ M^{-1} s^{-1}.

diffusion simulations under external drives show that the binding of Zn to Aβ in the synapse is minimal: ~0.001% of Aβ forms an Aβ-Zn complex from a single release of Zn, rising to ~0.1% of Aβ when Zn is released into the system at 100 Hz. Given the low probability of Aβ-Zn forming and its fast dissociation, this complex is unlikely to play a role in promoting Aβ dimer formation during neurotransmission in the synaptic cleft, a critical step for Aβ oligomerization. We suggest that the role of Zn may instead be associated with its ability to strongly influence Aβ in the late-stages of Aβ aggregation, such as the assembly of fibrils, which has been reported recently.[47] Binding of Cu to Aβ, in contrast, is much more likely, with 0.1% of Aβ forming Aβ-Cu during a single Cu release rising to ~30% of Aβ when Cu is released at a frequency of 100 Hz.

During low frequency repetitive releases of Cu, the ratio of $(A\beta\text{-Cu})_I$ to $(A\beta\text{-Cu})_{II}$ rises slightly from its equilibrium value of 71:29 to 75:25. Competition with other Cu binding proteins in the synapse such as HSA could increase this ratio even further, as HSA extracts Cu from $(A\beta\text{-Cu})_I$ on the same time scale (hundreds of milliseconds) as $(AB\text{-Cu})_{II}$ is formed.[33] Overall, $(AB\text{-Cu})_I$ forms quickly, but Cu is sequestered by HSA before interconversion into $(AB\text{-Cu})_{II}$. This is important because of the differing reactivity between $(AB\text{-Cu})_I$ and $(AB\text{-Cu})_{II}$: i.e., enhanced $(A\beta\text{-Cu})_I$ formation relative to $(A\beta\text{-Cu})_{II}$ might need to be considered in quantitative modeling of Aβ dimerization in the synaptic cleft. Indeed, $(A\beta\text{-Cu})_I$ is much more reactive than $(A\beta\text{-Cu})_{II}$ in forming metal bridged dimers,[33,34] although it is not yet clear whether this is the kinetic determinant of Aβ aggregation, or whether dimerization goes via Aβ monomers bound with two Cu ions.[34,48] In parallel, an increased population of $(A\beta\text{-Cu})_I$ would potentially generate more reactive oxygen species (ROS) compared to $(A\beta\text{-Cu})_{II}$. The highly flexible coordination configuration of $(A\beta\text{-Cu})_I$ has a low thermodynamic barrier (30 kJ/mol^{-1}) to forming an intermediate state which in turn favors fast redox reactions to produce ROS.[49] Asp1, His13, and His14 were identified as the main Cu(I/II) coordination ligands in this highly reactive intermediate state.[50] Production of ROS from $(A\beta\text{-Cu})_{II}$ is slower as $(AB\text{-Cu})_{II}$ must convert to $(A\beta\text{-Cu})_I$ for the access to this intermediate before the reduction reaction can take place.[51]

There is much experimental evidence to indicate that the propensity of Aβ dimer formation is related to the redox reaction of the Aβ-Cu complex. Radical chain reactions catalyzed by Aβ-Cu can not only oxidize lipid and protein molecules[52,53] but also Aβ itself.[54] One such example is dityrosine cross-linking of the two Aβ monomers via covalent ortho−ortho coupling of two tyrosine residues under conditions of oxidative stress with elevated copper.[55] Covalently cross-linked dimers and trimers are difficult to degrade and therefore could serve as long-living "seeds" to induce Aβ aggregation. The vast difference in the toxicity observed between in vivo and in vitro Aβ oligomer samples has been attributed to tyrosine cross-linking under in vivo oxidative stress conditions.[56] Our simulations imply that such cross-linking could readily take place in the synaptic cleft as a

DOI: 10.1021/acschemneuro.7b00121
ACS Chem. Neurosci. 2017, 8, 1970−1979

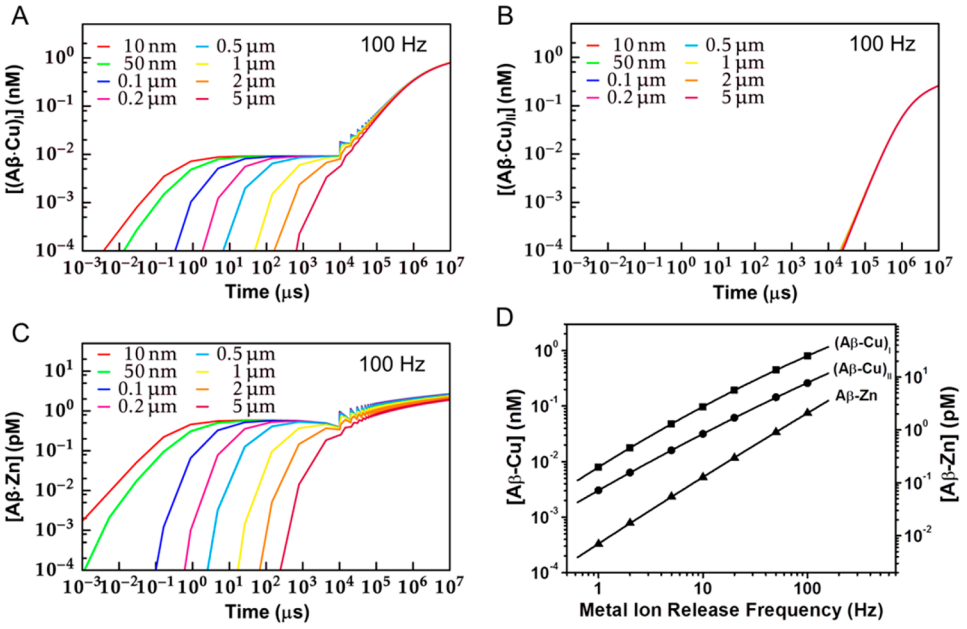

Figure 7. Reaction-diffusion simulation of metal binding to Aβ under repetitive metal release conditions (3 nM Aβ, 30 μM Cu, or 300 μM Zn). (A–C) Spatiotemporal profiles of (A) $(A\beta{\cdot}Cu)_I$, (B) $(A\beta{\cdot}Cu)_{II}$, and (C) Aβ·Zn concentrations at 100 Hz release frequency. (D) Mean concentration of Aβ·Cu and Aβ·Zn averaged over 300 nm width of the synaptic cleft after 10 s metal release at indicated frequencies. The solid lines are empirical fits.

substantial population of the Aβ here is associated with divalent Cu.

For simplicity, our simulations were carried out using deterministic reaction-diffusion equations under free diffusion conditions. However, the synapse and the vesicle carrying neurotransmitters are both small volumes: on average 0.6 Cu and 6 Zn ions will be released on each occasion, into synapses of which 1 in 400 will contain a single Aβ molecule (assuming a synapse diameter of 300 nm). Given these constraints, an alternative strategy would be to use a spatial stochastic model.[57,58] However, there are about 100 billion neurons in a human brain and each neuron has about 7000 synapses. Our primary interest is in assessing the differences between Cu and Zn binding to Aβ and the relative importance of the species formed, rather than estimating the fluctuations observed in individual synapses, determining the distribution of each outcome or investigating heterogeneity (as provided by stochastic simulation). To assess the behavior of a neuron, results from stochastic simulation would still need to be averaged and scaled by the probability of finding molecules in the small volume. Our simple continuous model captures this average behavior to a first approximation, and allows us to examine the spatiotemporal behavior of all synapses in an "average" of several neurons.

We have noticed a recent stochastic simulation of Cu-induced Aβ dimerization in a confined synaptic cleft.[59] In our opinion, it is essential to allow the metal ions to leave the synaptic cleft, since Zn and Cu are tightly regulated spatiotemporally for proper brain function.[21] The free diffusion to an open space employed in our simulation is an approximation of this biophysical requirement: in the absence of an open boundary, we would expect persistently high metal ion concentrations in the synapse cleft under sustained metal ion release and consequently all Aβ would become bound to metal ions.

Our results are also likely to be modified by the dense and viscous extracellular environment of the synaptic cleft. We attempted to estimate the extent of this effect by considering the likely changes in parameters of the simulations and how these would affect the numerical outcomes. It has been reported that the diffusion coefficient for small monovalent extracellular ions is reduced by a factor of 2.4 by tortuosity and volume fraction in the extracellular microenvironment of the rat cerebellum, though these ions still obey the laws of macroscopic diffusion.[60] It is also expected that Aβ molecules (molecular weight ~4 kDa) in the synaptic cleft would experience hindered diffusion with an effective diffusion coefficient around 2 to 3 times smaller than that used here.[61] Consequently the rate constant of the binding between the metal ions and Aβ would be reduced due to lower collision rates. The effect of this on the simulation result will be smaller than the effect of the change in diffusion coefficient because slower diffusion will reduce the dilution by diffusion of metal ions after release.

Membrane-bound Aβ molecules bind to metal ions at approximately the same rate as Aβ in free solution,[33] thus making our simulation results relevant to Aβ associated with neuronal membranes rich in ganglioside. GM1-bound Aβ has been proposed as an endogenous seed for Aβ amyloid in the brain.[62,63] Additionally, $(A\beta\text{-}Cu)_I$ formed on the membrane is likely to self-produce ROS locally damaging the unsaturated lipid and membrane protein.[53]

Together with our previous publications, we have characterized the kinetics of metal ion (Cu/Zn) binding to Aβ in detail. Cu binds Aβ with a rate constant ~5×10^8 M^{-1} s^{-1} and the $(A\beta\text{-}Cu)_I$ complex dissociates at 0.8 s^{-1}, while Zn binds considerably slower at ~2×10^6 M^{-1} s^{-1} and the complex dissociates at ~100 s^{-1}. The $(A\beta\text{-}Cu)_{II}$ complex is much more stable and its lifetime is governed by its rate of conversion (2.5 s^{-1}) to $(A\beta\text{-}Cu)_I$. Therefore, the Aβ-Cu and Aβ-Zn complexes can survive ~1 s and ~10 ms, respectively. Even for synaptic conditions where a single vesicle containing one or other ion may be released, this disparity in lifetime between the two complexes would greatly limit the formation of Zn associated

DOI: 10.1021/acschemneuro.7b00121
ACS Chem. Neurosci. 2017, 8, 1970–1979

Aβ dimer and leave less time for this metal-bound complex to reorganize to aggregation-prone conformations. Secondary binding reactions between Cu/Zn and Aβ-Cu are even slower, with rate constants on the order of 10^5 M^{-1} s^{-1} and 10^3 M^{-1} s^{-1} respectively. The reaction-diffusion simulations predict that only the Aβ-Cu complex will play a major role in the early stages of Aβ aggregation in the synaptic cleft, while other Aβ-metal complexes including Aβ-Zn are insignificant. In light of the recent finding that targeting Aβ aggregates is a promising approach for the treatment of AD,[64] we propose that drug development efforts for early stages of AD should aim to target the specific interactions between Cu and Aβ.

METHODS

Labeled Aβ. Aβ16 labeled by HiLyte Fluor 488 on lysine 16 (DAEFRHDSGYEVHHQK-HiLyte 488) was purchased from Anaspec (Fremont, CA) and dissolved in 50 mM HEPES (pH 7.5) and 100 mM NaCl. The purity, as determined by the percentage of peak area by HPLC, is greater than 95%. The concentrations of the peptide was measured via the peak absorbance of the dye (ε = 68 000 cm^{-1} M^{-1}) using a UV/vis spectrometer (Lambda 25, PerkinElmer, Wellesley, MA). Aβ was dissolved in a buffer solution containing 50 mM HEPES (pH 7.5). All buffers contain 100 mM NaCl. The stock solutions of labeled peptides were further diluted to nanomolar concentrations (50 nM) prior to the kinetic experiments.

Stopped-Flow Spectroscopy. Kinetics measurements were carried out using a KinetAsyst SF-610X2 stopped-flow spectrophotometer (HI-TECH Scientific, UK). Samples were excited either at 488 nm by a xenon lamp or at 473 nm by a fiber coupled diode laser (MCLS1-473-20, Thorlabs, Newton, NJ). All experiments were performed at 25 °C in 50 mM HEPES pH7.5, 100 mM NaCl, except where explicitly stated.

Kinetics of Zn Binding to Aβ. $CuCl_2$ (500 nM) was premixed with indicated concentrations of $ZnCl_2$ which were then mixed with 25 nM labeled Aβ using stopped-flow.

Kinetics of Zn Binding to Aβ-Cu. In this double jump experiment, 50 nM Aβ was first mixed with 100 nM $CuCl_2$. After an incubation time of 1 s, this was mixed with different concentrations of excess $ZnCl_2$ at the indicated temperatures (9−55 °C) and fluorescence recovery measured.

Multiple Cu Binding to Aβ. To determine the rate constants for the second Cu-binding event, 25 nM Ab was reacted with indicated concentrations of $CuCl_2$. To determine the rate constants of multiple Cu-binding reactions, 25 nM Aβ was premixed with indicated concentrations of $CuCl_2$ and the solutions then mixed with an equal volume of 4 mM EDTA in a double jump experiment.

Coupled Reaction-Diffusion Simulation. The simulation was based on a simplified cylindrical model of the synaptic cleft with a height of 20 nm. It is technically a 3D simulation, but we assumed that there is no concentration gradient in the 20 nm axial direction as the 20 nm radius vesicle would occupy the entire gap of the cleft. As a result, the simulation is simply 2D, and reduced to 1D in polar coordinates. The radius of the cylinder was assumed to be infinite so that the diffusion of metal ions released is not restricted to the typical synaptic width of a few hundred of nanometers. Metal ions (30 μM Cu^{2+} or 300 μM Zn^{2+}) were assumed to release into the center of the synapse via 40 nm diameter vesicles and react with 3 nM Aβ in the synaptic cleft. To simulate the periodic pulsed release of metal ions during neurotransmission, the concentration of metal ions at the center (20 nm radius) of each release was reset to initial concentration repeatedly at the particular frequency. The simulation code was written in C++. For more details, see the Supporting Information.

ASSOCIATED CONTENT

Supporting Information

The Supporting Information is available free of charge on the ACS Publications website at DOI: 10.1021/acschemneuro.7b00121.

Derivation of the apparent rate constant of Zn competing with Cu to bind Aβ, details of coupled reaction-diffusion simulations, temporal profiles of $(Aβ{\cdot}Cu)_I$, $(Aβ{\cdot}Cu)_{II}$, and Aβ·Zn concentrations (PDF)

AUTHOR INFORMATION

Corresponding Author

*E-mail: l.ying@imperial.ac.uk.

ORCID

Liming Ying: 0000-0001-9752-6292

Author Contributions

T.B., M.B., and L.Y. designed research; T.B. performed research; T.B., C.A.D., M.B., and L.Y. analyzed data; and T.B., C.A.D., and L.Y. wrote the paper.

Funding

This work was supported by the Engineering and Physical Sciences Research Council (EPSRC) and the Biotechnology and Biological Sciences Research Council (BBSRC) via the award of a Ph.D. studentship to T.B. under the Institute of Chemical Biology Doctoral Training Centre at Imperial College London, by the Leverhulme Trust via a project grant (RPG-2015-345) to L.Y., and by Imperial College London/Wellcome Trust ISSF via a Value in People Award to C.A.D.

Notes

The authors declare no competing financial interest.

REFERENCES

(1) Ross, C. A., and Poirier, M. A. (2004) Protein aggregation and neurodegenerative disease. *Nat. Med. 10*, S10−S17.

(2) Karran, E., Mercken, M., and De Strooper, B. (2011) The amyloid cascade hypothesis for Alzheimer's disease: an appraisal for the development of therapeutics. *Nat. Rev. Drug Discovery 10*, 698−712.

(3) Bush, A. I. (2003) The metallobiology of Alzheimer's disease. *Trends Neurosci. 26*, 207−214.

(4) Bush, A. I., and Tanzi, R. E. (2008) Therapeutics for Alzheimer's disease based on the Metal Hypothesis. *Neurotherapeutics 5*, 421−432.

(5) Walsh, D. M., and Selkoe, D. J. (2007) Aβ Oligomers - a decade of discovery. *J. Neurochem. 101*, 1172−1184.

(6) Benilova, I., Karran, E., and De Strooper, B. (2012) The toxic Aβ oligomer and Alzheimer's disease: an emperor in need of clothes. *Nat. Neurosci. 15*, 349−357.

(7) Watts, J. C., Condello, C., Stöhr, J., Oehler, A., Lee, J., DeArmond, S. J., Lannfelt, L., Ingelsson, M., Giles, K., and Prusiner, S. B. (2014) Serial propagation of distinct strains of Aβ prions from Alzheimer's disease patients. *Proc. Natl. Acad. Sci. U. S. A. 111*, 10323−10328.

(8) Stöhr, J., Condello, C., Watts, J. C., Bloch, L., Oehler, A., Nick, M., DeArmond, S. J., Giles, K., DeGrado, W. F., and Prusiner, S. B. (2014) Distinct synthetic Aβ prion strains producing different amyloid deposits in bigenic mice. *Proc. Natl. Acad. Sci. U. S. A. 111*, 10329−10334.

(9) Cohen, S. I. A., Linse, S., Luheshi, L. M., Hellstrand, E., White, D. A., Rajah, L., Otzen, D. E., Vendruscolo, M., Dobson, C. M., and Knowles, T. P. J. (2013) Proliferation of amyloid-beta 42 aggregates occurs through a secondary nucleation mechanism. *Proc. Natl. Acad. Sci. U. S. A. 110*, 9758−9763.

DOI: 10.1021/acschemneuro.7b00121
ACS Chem. Neurosci. 2017, 8, 1970−1979

(10) Michaels, T. C. T., Lazell, H. W., Arosio, P., and Knowles, T. P. J. (2015) Dynamics of protein aggregation and oligomer formation governed by secondary nucleation. *J. Chem. Phys. 143*, 054901.
(11) Pedersen, J. T., Ostergaard, J., Rozlosnik, N., Gammelgaard, B., and Heegaard, N. H. H. (2011) Cu(II) mediates kinetically distinct, non-amyloidogenic aggregation of amyloid-beta peptides. *J. Biol. Chem. 286*, 26952−26963.
(12) Faller, P., Hureau, C., and Berthoumieu, O. (2013) Role of metal ions in the self-assembly of the Alzheimer's amyloid-beta peptide. *Inorg. Chem. 52*, 12193−12206.
(13) Viles, J. H. (2012) Metal ions and amyloid fibre formation in neurodegenerative diseases. Copper, zinc and iron in Alzheimer's, Parkinson's and prion diseases. *Coord. Chem. Rev. 256*, 2271−2284.
(14) Pedersen, J. T., Borg, C. B., Michaels, T. C. T., Knowles, T. P. J., Faller, P., Teilum, K., and Hemmingsen, L. (2015) Aggregation-prone amyloid-β-Cu(II) species formed on the millisecond timescale under mildly acidic conditions. *ChemBioChem 16*, 1293−1297.
(15) Abelein, A., Graslund, A., and Danielsson, J. (2015) Zinc as chaperone-mimicking agent for retardation of amyloid beta peptide fibril formation. *Proc. Natl. Acad. Sci. U. S. A. 112*, 5407−5412.
(16) Hane, F., and Leonenko, Z. (2014) Effect of metals on kinetic pathways of amyloid-beta aggregation. *Biomolecules 4*, 101−116.
(17) Huang, X. D., Atwood, C. S., Moir, R. D., Hartshorn, M. A., Tanzi, R. E., and Bush, A. I. (2004) Trace metal contamination initiates the apparent auto-aggregation, amyloidosis, and oligomerization of Alzheimer's Aβ peptides. *JBIC, J. Biol. Inorg. Chem. 9*, 954−960.
(18) Frederickson, C. J., Giblin, L. J., Krezel, A., McAdoo, D. J., Muelle, R. N., Zeng, Y., Balaji, R. V., Masalha, R., Thompson, R. B., Fierke, C. A., Sarvey, J. M., de Valdenebro, M., Prough, D. S., and Zornow, M. H. (2006) Concentrations of extracellular free zinc (pZn)e in the central nervous system during simple anesthetization, ischemia and reperfusion. *Exp. Neurol. 198*, 285−293.
(19) Smith, D. G., Cappai, R., and Barnham, K. J. (2007) The redox chemistry of the Alzheimer's disease amyloid-β peptide. *Biochim. Biophys. Acta, Biomembr. 1768*, 1976−1990.
(20) Faller, P., and Hureau, C. (2009) Bioinorganic chemistry of copper and zinc ions coordinated to amyloid-β peptide. *Dalton Trans.*, 1080−1094.
(21) Tamano, H., and Takeda, A. (2011) Dynamic action of neurometals at the synapse. *Metallomics 3*, 656−661.
(22) Zawisza, I., Rózga, M., and Bal, W. (2012) Affinity of copper and zinc ions to proteins and peptides related to neurodegenerative conditions (Aβ, APP, α-synuclein, PrP). *Coord. Chem. Rev. 256*, 2297−2307.
(23) Alies, B., Renaglia, E., Rózga, M., Bal, W., Faller, P., and Hureau, C. (2013) Cu(II) affinity for the Alzheimer's peptide: tyrosine fluorescence studies revisited. *Anal. Chem. 85*, 1501−1508.
(24) Noel, S., Rodriguez, S. B., Sayen, S., Guillon, E., Faller, P., and Hureau, C. (2014) Use of a new water-soluble Zn sensor to determine Zn affinity for the amyloid-β peptide and relevant mutants. *Metallomics 6*, 1220−1222.
(25) Leal, S. S., Botelho, H. M., and Gomes, C. M. (2012) Metal ions as modulators of protein conformation and misfolding in neurodegeneration. *Coord. Chem. Rev. 256*, 2253−2270.
(26) Crouch, P. J., and Barnham, K. J. (2012) Therapeutic redistribution of metal ions to treat Alzheimer's disease. *Acc. Chem. Res. 45*, 1604−1611.
(27) Pithadia, A. S., and Lim, M. H. (2012) Metal-associated amyloid-beta species in Alzheimer's disease. *Curr. Opin. Chem. Biol. 16*, 67−73.
(28) Faller, P. (2009) Copper and zinc binding to amyloid-beta: coordination, dynamics, aggregation, reactivity and metal-Ion transfer. *ChemBioChem 10*, 2837−2845.
(29) Damante, C. A., Ösz, K., Nagy, Z., Grasso, G., Pappalardo, G., Rizzarelli, E., and Sóvágó, I. (2011) Zn^{2+}'s ability to alter the distribution of Cu^{2+} among the available binding sites of Aβ(1−16)-polyethylenglycol-ylated peptide: implications in Alzheimer's disease. *Inorg. Chem. 50*, 5342−5350.
(30) Silva, K. I., and Saxena, S. (2013) Zn(II) ions substantially perturb Cu(II) ion coordination in amyloid-β at physiological pH. *J. Phys. Chem. B 117*, 9386−9394.
(31) Alies, B., Sasaki, I., Proux, O., Sayen, S., Guillon, E., Faller, P., and Hureau, C. (2013) Zn impacts Cu coordination to amyloid-β, the Alzheimer's peptide, but not the ROS production and the associated cell toxicity. *Chem. Commun. 49*, 1214−1216.
(32) Klementieva, O., Willén, K., Martinsson, I., Israelsson, B., Engdahl, A., Cladera, J., Uvdal, P., and Gouras, G. K. (2017) Pre-plaque conformational changes in Alzheimer's disease-linked Aβ and APP. *Nat. Commun. 8*, 14726.
(33) Branch, T., Girvan, P., Barahona, M., and Ying, L. M. (2015) Introduction of a fluorescent probe to amyloid-β to reveal kinetic insights into its interactions with Copper(II). *Angew. Chem., Int. Ed. 54*, 1227−1230.
(34) Girvan, P., Miyake, T., Teng, X., Branch, T., and Ying, L. M. (2016) Kinetics of the interactions between copper and amyloid-β with FAD mutations and phosphorylation at the N-terminus. *ChemBioChem 17*, 1732−1737.
(35) Tõugu, V., Tiiman, A., and Palumaa, P. (2011) Interactions of Zn(II) and Cu(II) ions with Alzheimer's amyloid-beta peptide. Metal ion binding, contribution to fibrillization and toxicity. *Metallomics 3*, 250−261.
(36) Talmard, C., Bouzan, A., and Faller, P. (2007) Zinc binding to amyloid-beta: Isothermal titration calorimetry and Zn competition experiments with Zn sensors. *Biochemistry 46*, 13658−13666.
(37) Damante, C. A., Ösz, K., Nagy, Z., Pappalardo, G., Grasso, G., Impellizzeri, G., Rizzarelli, E., and Sóvágó, I. (2008) The metal loading ability of β-amyloid N-terminus: a combined potentiometric and spectroscopic study of copper(II) complexes with β-amyloid(1−16), its Short or mutated peptide fragments, and its polyethylene glycol (PEG)-ylated analogue. *Inorg. Chem. 47*, 9669−9683.
(38) Guilloreau, L., Damian, L., Coppel, Y., Mazarguil, H., Winterhalter, M., and Faller, P. (2006) Structural and thermodynamical properties of CuII amyloid-β16/28 complexes associated with Alzheimer's disease. *JBIC, J. Biol. Inorg. Chem. 11*, 1024−1038.
(39) Savtchenko, L. P., and Rusakov, D. A. (2007) The optimal height of the synaptic cleft. *Proc. Natl. Acad. Sci. U. S. A. 104*, 1823−1828.
(40) Qu, L., Akbergenova, Y., Hu, Y. M., and Schikorski, T. (2009) Synapse-to-synapse variation in mean synaptic vesicle size and its relationship with synaptic morphology and function. *J. Comp. Neurol. 514*, 343−352.
(41) Kariuki, S., and Dewald, H. D. (1996) Evaluation of diffusion coefficients of metallic ions in aqueous solutions. *Electroanalysis 8*, 307−313.
(42) Giedraitis, V., Sundelöf, J., Irizarry, M. C., Gårevik, N., Hyman, B. T., Wahlund, L. O., Ingelsson, M., and Lannfelt, L. (2007) The normal equilibrium between CSF and plasma amyloid beta levels is disrupted in Alzheimer's disease. *Neurosci. Lett. 427*, 127−131.
(43) Vogel, S. (1988) *Life's Devices: The Physical World of Animals and Plants*, Princeton University Press, Princeton, NJ.
(44) Rózga, M., Sokołowska, M., Protas, A. M., and Bal, W. (2007) Human serum albumin coordinates Cu(II) at its N-terminal binding site with 1 pM affinity. *JBIC, J. Biol. Inorg. Chem. 12*, 913−918.
(45) Rózga, M., and Bal, W. (2010) The Cu(II)/Aβ/human serum albumin model of control mechanism for copper-related amyloid neurotoxicity. *Chem. Res. Toxicol. 23*, 298−308.
(46) Attwell, D., and Gibb, A. (2005) Neuroenergetics and the kinetic design of excitatory synapses. *Nat. Rev. Neurosci. 6*, 841−849.
(47) Matheou, C. J., Younan, N. D., and Viles, J. H. (2016) The rapid exchange of $zinc^{2+}$ enables trace levels to profoundly influence amyloid-beta misfolding and dominates assembly outcomes in Cu^{2+}/Zn^{2+} mixtures. *J. Mol. Biol. 428*, 2832−2846.
(48) Pedersen, J. T., Teilum, K., Heegaard, N. H. H., Østergaard, J., Adolph, H. W., and Hemmingsen, L. (2011) Rapid formation of a preoligomeric peptide−metal−peptide complex following copper(II) binding to amyloid β peptides. *Angew. Chem., Int. Ed. 50*, 2532−2535.

DOI: 10.1021/acschemneuro.7b00121
ACS Chem. Neurosci. 2017, 8, 1970−1979

(49) Balland, V., Hureau, C., and Savéant, J. M. (2010) Electrochemical and homogeneous electron transfers to the Alzheimer amyloid-β copper complex follow a preorganization mechanism. *Proc. Natl. Acad. Sci. U. S. A. 107*, 17113−17118.
(50) Cassagnes, L.-E., Hervé, V., Nepveu, F., Hureau, C., Faller, P., and Collin, F. (2013) The catalytically active copper-amyloid-beta state: coordination site responsible for reactive oxygen species production. *Angew. Chem., Int. Ed. 52*, 11110−11113.
(51) Furlan, S., Hureau, C., Faller, P., and La Penna, G. (2012) Modeling copper binding to the amyloid-β peptide at different pH: toward a molecular mechanism for Cu reduction. *J. Phys. Chem. B 116*, 11899−11910.
(52) Butterfield, D. A., Reed, T., Newman, S. F., and Sultana, R. (2007) Roles of amyloid β-peptide associated oxidative stress and brain protein modifications in the pathogenesis of Alzheimer's disease and mild cognitive impairment. *Free Radical Biol. Med. 43*, 658−677.
(53) Butterfield, D. A., Swomley, A. M., and Sultana, R. (2013) Amyloid β-peptide (1−42) induced oxidative stress in Alzheimer disease: importance in disease pathogenesis and progression. *Antioxid. Redox Signaling 19*, 823−835.
(54) Barnham, K. J., Haeffner, F., Ciccotosto, G. D., Curtain, C. C., Tew, D., Mavros, C., Beyreuther, K., Carrington, D., Masters, C. L., Cherny, R. A., Roberto Cappai, R., and Bush, A. I. (2004) Tyrosine gated electron transfer is key to the toxic mechanism of Alzheimer's disease β-amyloid. *FASEB J. 18*, 1427−1429.
(55) Al-Hilaly, Y. K., Williams, T. L., Stewart-Parker, M., Ford, L., Skaria, E., Cole, M., Bucher, W. G., Morris, K. L., Sada, A. A., Thorpe, J. R., and Serpell, L. C. (2013) A central role for dityrosine crosslinking of Amyloid-β in Alzheimer's disease. *Acta Neuropathol. Commun. 1*, 83.
(56) Sitkiewicz, E., Olędzki, J., Poznański, J., and Dadlez, M. (2014) Di-tyrosine cross-link decreases the collisional cross-section of Aβ peptide dimers and trimers in the gas phase: an ion mobility study. *PLoS One 9*, e100200.
(57) Gillespie, D. T. (2007) Stochastic simulation of chemical kinetics. *Annu. Rev. Phys. Chem. 58*, 35−55.
(58) Grima, R., and Schnell, S. (2008) Modelling reaction kinetics inside cells. *Essays Biochem. 45*, 41−56.
(59) Goch, W., and Bal, W. (2017) Numerical simulations reveal randomness of Cu(II) induced Aβ peptide dimerization under conditions present in glutamatergic synapses. *PLoS One 12*, e0170749.
(60) Nicholson, C., and Phillips, J. M. (1981) Ion diffusion modified by tortuosity and volume fraction in the extracellular microenvironment of the rat cerebellum. *J. Physiol. 321*, 225−257.
(61) Nicholson, C., and Tao, L. (1993) Hindered diffusion of high molecular weight compounds in brain extracellular microenvironment measured with integrative optical imaging. *Biophys. J. 65*, 2277−2290.
(62) Kakio, A., Nishimoto, S., Yanagisawa, K., Kozutsumi, Y., and Matsuzaki, K. (2001) Cholesterol-dependent formation of GM1 ganglioside-bound amyloid beta-protein, an endogenous seed for Alzheimer amyloid. *J. Biol. Chem. 276*, 24985−24990.
(63) Hayashi, H., Kimura, N., Yamaguchi, H., Hasegawa, K., Yokoseki, T., Shibata, M., Yamamoto, N., Michikawa, M., Yoshikawa, Y., Terao, K., Matsuzaki, K., Lemere, C. A., Selkoe, D. J., Naiki, H., and Yanagisawa, K. (2004) A seed for Alzheimer amyloid in the brain. *J. Neurosci. 24*, 4894−4902.
(64) Sevigny, J., Chiao, P., Bussière, T., Weinreb, P. H., Williams, L., Maier, M., Dunstan, R., Salloway, S., Chen, T., Ling, Y., O'Gorman, J., Qian, F., Arastu, M., Li, M., Chollate, S., Brennan, M. S., Quintero-Monzon, O., Scannevin, R. H., Arnold, H. M., Engber, T., Rhodes, K., Ferrero, J., Hang, Y., Mikulskis, A., Grimm, J., Hock, C., Nitsch, R. M., and Sandrock, A. (2016) The antibody aducanumab reduces Aβ plaques in Alzheimer's disease. *Nature 537*, 50−56.

DOI: 10.1021/acschemneuro.7b00121
ACS Chem. Neurosci. 2017, 8, 1970−1979